

## Resonant Formation and Control of 2D Symmetric Vortex Waves

L. Friedland<sup>1</sup> and A. G. Shagalov<sup>2</sup>

<sup>1</sup>*Racah Institute of Physics, Hebrew University of Jerusalem, Jerusalem 91904, Israel*

<sup>2</sup>*Institute of Metal Physics, Ekaterinburg 620219, Russian Federation*

(Received 29 March 2000)

It is shown that  $m$ -fold symmetric vortex waves in two dimensions ( $V$  states) preserve their functional form in a weak straining flow having appropriate symmetry, but arbitrary time dependence. This phenomenon is used in driving the  $V$  states into a highly nonlinear excitation by subjecting a circular vortex patch to rotation and strain with oscillating strain rate and varying the rotation angular velocity. The effect is due to autoresonance in the system as the excited vortex state boundary self-adjusts its aspect ratio to synchronize with the external flow.

PACS numbers: 47.32.Cc

The  $V$  states, discovered by Deem and Zabusky [1], comprise uniformly rotating, shape preserving vortex patch solutions of two-dimensional Euler equations. They are  $m$ -fold symmetric generalizations of the elliptic Kirchhoff vortices [2] having constant vorticity and twofold symmetry. The form of the  $V$  states is given by an integrodifferential equation [1,3], yielding, for each  $m$ , a family of solutions depending on a single parameter (say, the rotation frequency  $\Omega_m$  of the patch). Numerical studies of  $V$  states via contour dynamics (CD) algorithm [1] showed that the vortex boundary remains stable with the decrease of its rotation frequency, until some critical  $\Omega_m$ , when the  $V$  state transforms into a curvilinear polygon with included angles of  $\pi/2$  [4], and there exist no  $V$  states for  $\Omega_m$  below the critical.

Since their discovery, the  $V$  states are frequently viewed as examples of dispersive nonlinear waves associated with a more general problem of interface dynamics subject to a global constraint (conservation of the enclosed area, for example). Related nonlinear wave forms on a closed interface are known in a variety of physical systems such as liquid drops [5], two-dimensional electron systems in a magnetic field [6], and non-neutral plasmas [7], to name just a few examples. The analysis of shape preserving rotating equilibria in these systems is usually based on either CD simulations, or various *local* models of closed curve dynamics in the plane [6,8]. These approaches yield many interesting solutions, but there exists no simple general way of realizing these solutions experimentally. In this Letter, we propose to combine external resonant perturbations with a variation of system parameters for *autoresonant* formation and control of shape preserving modes in interface dynamics, while starting from simple (experimentally realizable) equilibria. The autoresonance, best known from applications in particle accelerators [9], was recently used in manipulating rotating modes in non-neutral plasma experiments [10]. It was also suggested as a method for generating solitons [11], and Kirchhoff vortices [12]. The present study applies an autoresonant control idea to all  $V$  states.

We proceed from numerical illustrations of our approach. Consider a vortex patch having constant vortic-

ity  $\omega$  and a circular cross section of radius  $a$  at some initial time  $t_0$ . We subject the vortex to external strain and rotation of form  $dx/dt = \partial\psi/\partial y - \Omega(t)y$ ,  $dy/dt = -\partial\psi/\partial x + \Omega(t)x$ . Here the stream function in polar coordinates is  $\psi = \varepsilon(t)R^2(r/R)^m \cos(m\varphi)$ , a natural choice in the case of  $m$ -fold symmetric boundary conditions on a coaxial cylinder of radius  $R > a$ . The rotation frequency  $\Omega$  and/or the strain rate  $\varepsilon$  are time dependent, but  $\varepsilon$  is small enough (see below) to view the strain contribution to vortex dynamics as a perturbation.

Figure 1 shows the results of CD simulations of evolution of the driven vortex patch for  $m = 3, 4$ , and  $5$ . In these examples the strain rate was constant, while the rotation frequency varied linearly in time,  $\Omega(t) = -\Omega_{m0} - \alpha t$ , where  $\Omega_{m0} = \omega(m-1)/2m$  was the angular velocity of a weak  $m$ -fold symmetric disturbance of the circular vortex boundary [4]. The external rotation cancels the self-rotation of the  $m$ -fold disturbance at  $t = 0$  in this case. For convenience, we introduce dimensionless time  $\tau = \alpha^{1/2}t$  in our calculations and use dimensionless  $x, y, r, \varepsilon$ ,

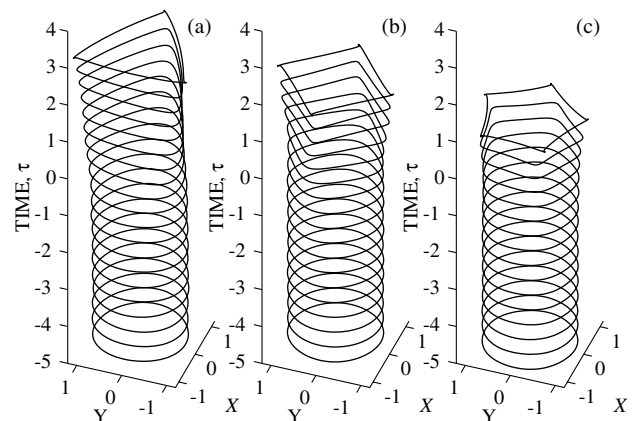


FIG. 1. The evolution of the strained  $V$ -state boundary in CD simulations with linearly chirped external rotation frequency. (a)  $m = 3$ , normalized strain rate  $\mu = 0.06$ ; (b)  $m = 4$ ,  $\mu = 0.03$ ; (c)  $m = 5$ ,  $\mu = 0.02$ . Each example develops cusps after passing a curvilinear polygon stage.

$\Omega$ ,  $\Omega_{m0}$ , and  $\omega$ , representing  $x/a$ ,  $y/a$ ,  $r/a$ ,  $\alpha^{-1/2}\varepsilon$ ,  $\alpha^{-1/2}\Omega$ ,  $\alpha^{-1/2}\Omega_{m0}$ , and  $\alpha^{-1/2}\omega$  in original notations. Then  $\Omega(\tau) = -\Omega_{m0} - \tau$ . Figures 1a–1c show the evolution of the patch boundary starting from a circle at initial  $\tau_0 = -5$ . The dimensionless strain parameter  $\mu = \varepsilon\alpha^{-1/2}(a/R)^{m-2}$  in these calculations was 0.06, 0.03, and 0.02 (for  $m = 3, 4$ , and  $5$ , respectively), while (dimensionless)  $\omega = -100$ . We observe excitation of  $V$  states of growing amplitude in the figure in all three examples at  $\tau > 0$ , i.e., beyond the linear resonance. These states are nearly stationary, as the external rotation cancels (resonates with) the natural rotation of the  $V$  state continuously. The deviation of the  $V$  states from the circle increases with the decrease of the external rotation frequency as the system self-preserved the resonance, until at  $\tau \approx 3, 2$ , and  $1$  (for  $m = 3, 4$ , and  $5$ , respectively) the contours transform into curvilinear polygons. Soon after, as the decrease of the external rotation frequency continues, the vortices develop cusps at polygon corners and the phase locking with the external rotation discontinues. We used a standard CD algorithm [13,14] with 120 initially equally spaced points on the contour in each simulation. The accuracy was tested by both doubling the number of points on the contour and decreasing the integration time step, and checking the absence of visible changes in the results shown in Fig. 1.

Additional details from our simulations in the  $m = 3$  case are presented in Fig. 2, showing (circles) the aspect ratio  $\gamma = r_{\max}/r_{\min}$ , and the inclination angle  $\Theta$  of the vortex patch ( $\Phi = m\Theta$  in the figure), defined as the angular coordinate of the maximum radius  $r_{\max}$  of the patch in the sector  $|\varphi| < \pi/m$  in the rest frame. The full lines in the figure correspond to the results obtained from our analytic theory [solutions of Eqs. (12) and (13)]. The evolution for other  $m$  was similar. One can see in the figure the phase

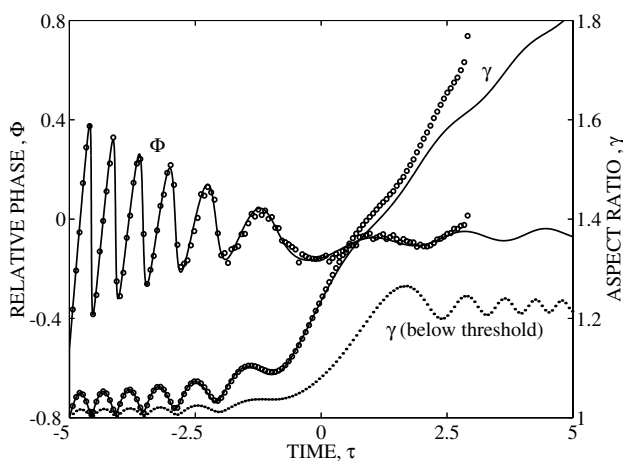


FIG. 2. The relative phase  $\Phi = m\Theta$  and the aspect ratio  $\gamma = r_{\max}/r_{\min}$  of the vortex patch versus time  $\tau$  for the  $m = 3$  example shown in Fig. 1. (Circles): Data based on CD simulations; (lines): solutions of systems (12) and (13); (dots): CD simulations for the same parameters, but  $\mu = 0.02$ , i.e., below the threshold for autoresonance.

locking near  $\Theta \approx 0$  and relatively rapid excitation of the  $V$  state beyond  $\tau = 0$ , as the vortex adjusts its angular velocity to stay in resonance with the external rotation. Also, in autoresonance, both the aspect ratio and  $\Theta$  perform small autoresonant oscillations around monotonically varying averages. Another characteristic of autoresonance is that entering the continuing nonlinear phase locking stage by passage through linear resonance in the system has a threshold  $\varepsilon_{\text{th}}$  on the strain rate. The dotted line in Fig. 2 represents simulation results for the same initial conditions and parameters as the circles, but with  $\mu = 0.02$ , which is below the theoretical threshold value of 0.027 in this case [see Eq. (14)]. In addition to the results displayed in Figs. 1 and 2, we found that the  $V$  states can be excited without using external rotation, but by oscillating the strain rate instead. We have used  $\varepsilon = \bar{\varepsilon} \cos[m\Psi(\tau)]$  and chirped the oscillation frequency  $d\Psi(\tau)/d\tau$  similarly to the rotation frequency above, i.e.,  $d\Psi/d\tau = -\Omega_{m0} - \tau$ . When  $\bar{\varepsilon}$  was *twice* the constant strain rate used with the varying external rotation, the vortex dynamics was almost identical to that shown in Fig. 1, but the excited  $V$  state was nearly stationary in the system rotating with the angular velocity of oscillations of the strain. Furthermore, we have found that, prior to large excitations leading to cusp formation, one can revert the excitation process and return the vortex to its nearly circular state by simply changing the direction of variation of the frequency of the external rotation or that of oscillations of the strain rate. This phenomenon is illustrated in Fig. 3, showing the evolution of the vortex patch in the  $m = 4$  case, for the same conditions as in Fig. 1, but periodically oscillating the external rotation frequency as  $\Omega(\tau) = -\Omega_{m0} + 2 - 3 \sin(\pi\tau/10)$ . Three stages of stable excitations and deexcitations of the  $V$  state can be seen in the figure during successive oscillation periods of  $\Omega(\tau)$ .

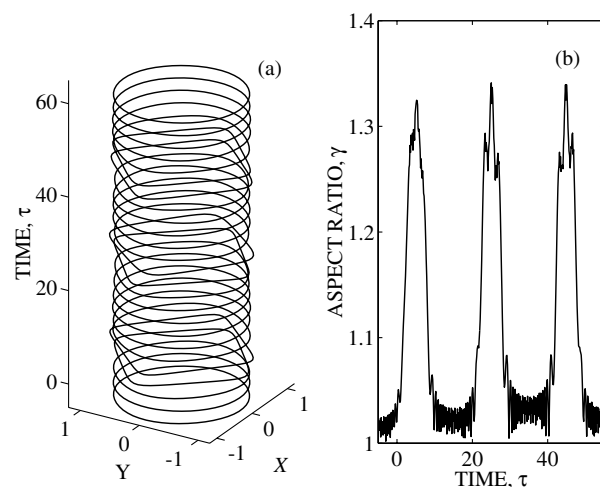


FIG. 3. Three successive excitations and deexcitations of the  $m = 4$   $V$  state in CD simulations with oscillating external rotation frequency. (a) Vortex boundary versus normalized time  $\tau$ ; (b) aspect ratio  $\gamma = r_{\max}/r_{\min}$  versus  $\tau$ .

Now we proceed to the theory of the phenomena illustrated above. Our starting point is the representation by Su [3] for the boundary of a free, weakly excited  $V$  state in polar coordinates  $(r', \varphi')$  attached to the vortex patch:

$$r' = p + \delta \cos m \varphi' + \frac{2m-1}{4p} \delta^2 \cos 2m \varphi' + O(\delta^3). \quad (1)$$

Here  $\delta$  measures the deviation from the circle, while  $p$  can be related to the area  $A = \pi a^2$  of the vortex patch, i.e.,  $p^2 = a^2 - \delta^2/2 + O(\delta^4)$ . Su also gives the angular rotation velocity of a weakly excited  $V$  state [3]:

$$\Omega_m = \Omega_{m0} - \frac{\omega(m-1)}{4p^2} \delta^2 + O(\delta^4). \quad (2)$$

We shall see that, under certain conditions,  $V$  states preserve their form (1) even if subjected to the  $m$ -fold symmetric external flow and rotation introduced above. Kida [15] showed that this statement is exact to all orders in  $\delta$  and for any  $\epsilon$ , i.e., that the elliptic vortex preserves its exact elliptic shape despite the strain and external rotation. We shall prove a similar statement for  $m > 2$ , but to  $O(\delta^2)$  in (1) and weak ( $\mu \ll 1$ ), but otherwise arbitrary, time dependent strain rate  $\epsilon(t)$ , thus generalizing Kida's result to all  $m$ . In other words, for  $\delta/a$  small enough, all  $V$  states subjected to the above-mentioned rotation and weak strain comprise a two parameter ( $\delta$ , and inclination angle  $\Theta$  of the coordinate system attached to the  $V$  state) family of solutions of form (1), with both  $\delta$  and  $\Theta$  being nontrivial functions of time.

In proving the aforementioned statement, we subject an  $m$ -fold symmetric  $V$  state to rotation and strain and seek a solution of form (1), for the vortex patch boundary. The parameters  $\delta$ ,  $p$ , and angle  $\Theta = \varphi - \varphi'$  in this solution are still unknown functions of time. We observe that if a point  $(\varphi', r')$  on the contour satisfies (1) at some initial time, say  $t_0$ , then the function  $F(r', \varphi'; t) \equiv p(t) + \delta(t) \cos m \varphi' + \frac{(2m-1)\delta^2(t)}{4p} \cos 2m \varphi' - r'$  vanishes at  $t_0$ . This function vanishes at later times as well, provided that the assumed form of the contour is preserved as the point moves with the flow. Thus, the kinematic condition of preservation of the functional form (1) of the vortex boundary is

$$\frac{dF}{dt} = \frac{\partial F}{\partial t} + \frac{\partial F}{\partial r} \frac{dr}{dt} + \frac{\partial F}{\partial \varphi} \frac{d\varphi}{dt} = 0, \quad (3)$$

where we transformed to the laboratory frame by replacing  $r' \rightarrow r$  and  $\varphi' \rightarrow \varphi - \Theta(t)$ , while the radial and azimuthal velocities  $dr/dt$  and  $d\varphi/dt$  of the point on the contour are due to the external rotation, strain, and the action of the vortex on itself:

$$dr/dt = -m\epsilon(t)R(r/R)^{m-1} \sin(m\varphi), \quad (4)$$

$$d\varphi/dt = \Omega + \Omega_m - m\epsilon(t)(r/R)^{m-2} \cos(m\varphi). \quad (5)$$

The substitution of these expressions into (3) yields

$$\frac{dp}{dt} + C \frac{d\delta}{dt} + mS\delta \left[ \frac{d\Theta}{dt} - \Omega - \Omega_m \right] = -\epsilon m p, \quad (6)$$

where  $C = \cos(m\varphi') + \frac{2m-1}{2p} \delta \cos(2m\varphi')$ ,  $S = \sin(m\varphi') + \frac{2m-1}{2p} \delta \sin(2m\varphi')$ , and

$$P = (r/R)^{m-2} [r \sin(m\varphi) + mS\delta \cos(m\varphi)]. \quad (7)$$

Next, we view  $\epsilon$  in (6) as small and, consequently, expand  $P$  on the right-hand side (RHS) in this equation to first order in  $\delta$ :

$$P \approx (p/R)^{m-2} \{ pS \cos(m\Theta) + [pC - \delta/2] \sin(m\Theta) \}. \quad (8)$$

Note that because of our special choice of the straining flow,  $P$  depends on  $\varphi'$  via  $S$  and  $C$  only in this lowest order approximation. As the result, one can equate the terms in (6) which are independent of  $\varphi'$ , as well as the coefficients of terms with  $C$  and  $S$ , to obtain the desired evolution equations for  $p$ ,  $\delta$ , and  $\Theta$ :

$$\frac{dp}{dt} = \epsilon m \left( \frac{p}{R} \right)^{m-2} \frac{\delta}{2} \sin(m\Theta), \quad (9)$$

$$\frac{d\delta}{dt} = -\epsilon m \left( \frac{p}{R} \right)^{m-2} p \sin(m\Theta), \quad (10)$$

$$\frac{d\Theta}{dt} = d - \frac{\omega(m-1)\delta^2}{4p^2} - \epsilon \left( \frac{p}{R} \right)^{m-2} \frac{p}{\delta} \cos(m\Theta), \quad (11)$$

where  $d = \Omega + \Omega_{m0}$ . This system is a weakly nonlinear,  $m$ -fold symmetric generalization of Kida's equations for unsteady strained elliptic vortices [15]. Note that Eqs. (9) and (10) can be combined to yield  $dp/dt = -(\delta/2p)(d\delta/dt)$ , or  $p^2 = a^2 - \delta^2/2$ , which, as expected, reflects the area conservation of the vortex patch (1) to desired order. Note also that for constant  $\epsilon$  and  $d$ , Eqs. (9)–(11) allow steady solutions with  $\Theta = 0$ , or  $\pi$  and  $\Delta = \delta/p$  satisfying a cubic equation,  $\frac{1}{4}\omega(m-1)\Delta^3 - d\Delta \pm \epsilon(p/R)^{m-2} = 0$ . This is a generalization of steady Moore-Saffman elliptic vortices [16] in a uniform shear flow. Next, we consider the unsteady evolution of the vortex, described by Eqs. (9)–(11). To lowest order, we substitute  $p \approx a$  in the RHS in Eqs. (10) and (11) and rewrite these equations for the linear chirp case,  $d = -\alpha t$ :

$$\frac{d\Delta}{d\tau'} = -\epsilon_0 \sin\Phi, \quad (12)$$

$$\frac{d\Phi}{d\tau'} = -\tau' + \omega_0 \Delta^2/8 - \epsilon_0 \Delta^{-1} \cos\Phi, \quad (13)$$

where  $\Delta \approx \delta/a$ ,  $\Phi = m\Theta$ , vorticity  $\omega$  is negative, and we introduce dimensionless time  $\tau' = (m\alpha)^{1/2} t$  and parameters  $\epsilon_0 = (m/\alpha)^{1/2} (a/R)^{m-2} \epsilon = m^{1/2} \mu$ ,  $\omega_0 = 2(m/\alpha)^{1/2} (m-1)|\omega|$ .

The systems (12) and (13) depend on the values of parameters  $\omega_0$  and  $\varepsilon_0$  only, so, when starting in a circular equilibrium, formation of  $V$  states proceeds similarly for all  $m$ . Consequently, in interpreting the results presented in Figs. 1–3, one can use recent theory [12], where equations similar to (12) and (13) were analyzed in application to driven Kirchhoff vortices ( $m = 2$   $V$  state). In particular, one finds that, above certain  $\varepsilon_0$ , the passage through resonance in Eqs. (12) and (13) yields persisting phase locking,  $\Phi \approx 0$ , while the nonlinear frequency shift adjusts automatically ( $\omega_0 \Delta^2/8 \approx \tau'$ , at  $\tau' > 0$ ) to preserve the resonance despite variation of the external rotation frequency. Formally, this solution corresponds to the adiabatic following of the aforementioned  $m$ -fold symmetric generalization of the quasisteady Moore-Saffman vortex, by starting from a circle at negative  $\tau'$  and choosing the solution branch with  $\Delta$  growing at all times. In addition to this adiabatic quasisteady state component, the actual solution also includes small autoresonant oscillations [12] of  $\Delta$  and  $\Phi$ , around the quasisteady state, as seen in Fig. 2. The threshold value on  $\varepsilon_0$  for entering this autoresonant state is  $\varepsilon_{0\text{th}} = (\frac{4}{3})^{3/4} \omega_0^{-1/2}$  [12] or, in original notations,

$$\mu_{\text{th}} \equiv \frac{\varepsilon_{\text{th}}}{\alpha^{1/2}} \left( \frac{a}{R} \right)^{m-2} = \frac{2\alpha^{1/4}}{(3m)^{3/4} [(m-1)|\omega|]^{1/2}}. \quad (14)$$

Note that the values of  $\delta$  for all  $m > 2$   $V$  states studied here are sufficiently small for using  $O(\delta^2)$  truncation in the driven  $V$ -states theory almost until the formation of the cusp [as illustrated by a good agreement between the solutions of Eqs. (12) and (13) and the CD simulation results in Fig. 2]. Finally, suppose one removes the external rotation, but oscillates instead the strain rate,  $\varepsilon_0 = \bar{\varepsilon}_0 \cos m\Psi$ , where the oscillation frequency is chirped as  $d\Psi/d\tau = -\Omega_{m0} - \tau$ . Then, by single resonance approximation in the interaction terms in Eqs. (10) and (11), one again reduces the problem to evolution equations (12) and (13) with  $\varepsilon_0$  replaced by  $\frac{1}{2}\bar{\varepsilon}_0$  and  $\Phi$  representing  $m(\Theta - \Psi)$ . This explains the aforementioned equivalence between varying the external rotation frequency or, alternatively, chirping the frequency of oscillations of the strain rate in controlling the vortex state.

In conclusion, we have presented theory and simulations of resonant formation and control of  $V$  states in incompressible fluids by starting in a circular equilibrium and using a weak strain of appropriate symmetry. We have shown that, similarly to Kida's strained elliptic vortices, the  $m > 2$   $V$  states preserve their functional form for sufficiently small excitations and weak strain rates of arbitrary time dependence. As the result, the driven vortex dynamics reduces to studying evolution of just two parameters (amplitude  $\delta$  and inclination angle  $\Theta$ ), while the imple-

mentation of the nonlinear phase locking (autoresonance) idea allows one to efficiently manipulate the vortex state. It seems interesting to apply a similar analysis to other classes of closed interface dynamics, to generalize the theory for use with nonuniform vorticity equilibria, and to develop higher dimensional analogs of the suggested nonlinear pattern formation process. Because of simple initial and boundary conditions in our approach, experimental realization of  $V$  states and other nontrivial nonlinear wave patterns in interface dynamics and their investigation may become feasible. For example, magnetized, pure electron plasmas can serve as a convenient experimental test ground for our theory. The equations governing these plasmas are isomorphic to those governing inviscid, incompressible, 2D fluids, with scaled plasma density playing the role of vorticity and scaled electric potential the role of the stream function in the fluid case. Thus, as in other recent experiments in electron plasmas [10], one can start with a simple, circular cross section plasma equilibrium and apply oscillating potentials on external confining walls, providing the straining flow analog of appropriate symmetry for studying driven  $V$ -state dynamics.

We acknowledge the support by the Israel Science Foundation (Grant No. 607-97) and by INTAS (Grant No. 99-1068).

- 
- [1] G. S. Deem and N. J. Zabusky, Phys. Rev. Lett. **40**, 859 (1978).
  - [2] H. Lamb, *Hydrodynamics* (Cambridge University Press, Cambridge, 1932), 6th ed., p. 173.
  - [3] C. H. Su, Phys. Fluids **22**, 2032 (1979).
  - [4] P. G. Saffman, *Vortex Dynamics* (Cambridge University Press, Cambridge, 1992), Sect. 9.4.
  - [5] A. Ludu and J. P. Draayer, Phys. Rev. Lett. **80**, 2125 (1998).
  - [6] C. Wexler and A. T. Dorsey, Phys. Rev. Lett. **82**, 620 (1999).
  - [7] J. Fajans, E. Yu. Backhaus, and J. E. McCarthy, Phys. Plasmas **6**, 12 (1999).
  - [8] R. E. Goldstein and D. M. Petrich, Phys. Rev. Lett. **67**, 3203 (1991).
  - [9] M. S. Livingston, *High Energy Accelerators* (Interscience, New York, 1954).
  - [10] J. Fajans, E. Gilson, and L. Friedland, Phys. Rev. Lett. **82**, 4444 (1999).
  - [11] L. Friedland and A. G. Shagalov, Phys. Rev. Lett. **81**, 4357 (1998).
  - [12] L. Friedland, Phys. Rev. E **59**, 4106 (1999).
  - [13] N. J. Zabusky, M. H. Hughes, and K. V. Roberts, J. Comput. Phys. **30**, 96 (1979).
  - [14] D. G. Dritschel, Comput. Phys. Rep. **10**, 77 (1989).
  - [15] S. Kida, J. Phys. Soc. Jpn. **50**, 3517 (1981).
  - [16] D. W. Moore and P. G. Saffman, *Aircraft Wake Turbulence and Its Detection* (Plenum Press, New York, 1971), p. 339.